

# The Radon Transform: A New Scheme for Fast Multidimensional NMR

ERIKS KUPČE,<sup>1</sup> RAY FREEMAN<sup>2</sup>

<sup>1</sup> Varian, Ltd., 28 Manor Road, Walton-on-Thames, Surrey KT12 2QF, United Kingdom

<sup>2</sup> Jesus College, Cambridge CB5 8BL, United Kingdom

**ABSTRACT:** Multidimensional nuclear magnetic resonance (NMR) spectra are used widely for structure elucidation of molecules of biochemical interest, particularly proteins, but the existing methodology is severely hampered by the long duration of the measurement, often many days. Here, we show that the inverse Radon transform can be used to reconstruct such a spectrum from a small number of different plane projections. This “projection-reconstruction” (PR) technique reduces the time required to perform a three-dimensional experiment by an order of magnitude and four-dimensional spectra by two orders of magnitude, greatly extending the scope of such investigations. We show the application of the inverse Radon transform to reconstruct the four-dimensional NMR spectrum of the nuclease A inhibitor, a measurement completed in only 35 min. This new technique is expected to have wide implications for investigations of protein structure and dynamics, currently a very active field of research. © 2004 Wiley Periodicals, Inc. Concepts Magn Reson Part A 22A: 4–11, 2004

**KEY WORDS:** Radon transform; multidimensional spectroscopy; projection-reconstruction; back-projection; nuclease A inhibitor

## INTRODUCTION

For many years, the practice of nuclear magnetic resonance (NMR) spectroscopy has been dominated virtually exclusively by the use of the Fourier transform (1). We draw attention here to the advantages of using the Radon transform (2) in multidimensional

NMR spectroscopy. The Radon procedure calculates multiple line integrals of the absorption along parallel paths (beams) through the sample and repeats the process for a set of different angles of incidence arranged around a circle. The Radon *transform* converts these line integrals into a related set of projections at right angles to the original beams.

Received 9 December 2003; accepted 12 December 2003

Correspondence to: Ray Freeman; E-mail: rf110@hermes.cam.ac.uk

Concepts in Magnetic Resonance Part A, Vol. 22A(1) 4–11 (2004)

Published online in Wiley InterScience (www.interscience.wiley.com). DOI 10.1002/cmra.20006

© 2004 Wiley Periodicals, Inc.

$$R(p, \phi) = \iint f(xy) \delta(x \cos \phi + y \sin \phi - p) dx dy, \quad [1]$$

where  $p$  is the perpendicular distance of the beam from the origin and  $\phi$  is the angle of incidence of the

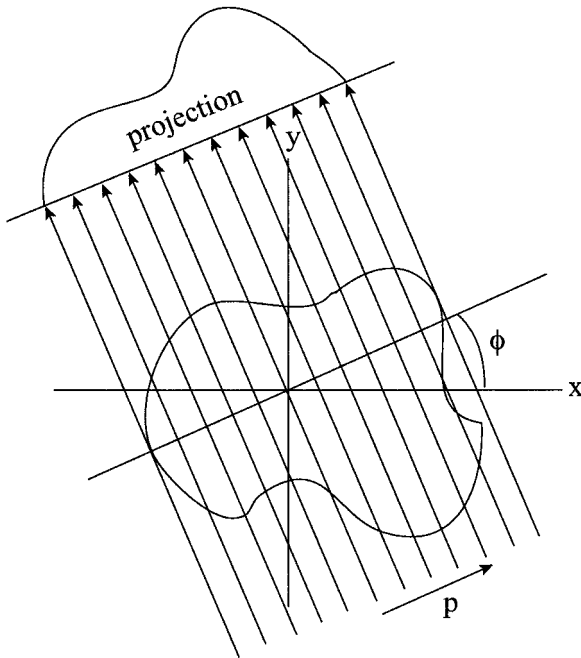


**Figure 1** The Radon transform computes the projection of the absorption intensity onto an axis defined by the angle  $\phi$ , by taking the integrals along a set of parallel beams offset at regularly increasing distances  $p$  from the origin. Because of this integration, the *inverse* Radon transform cannot be performed for a single value of  $\phi$ , but becomes feasible if a large number of values of  $\phi$  are used. In this manner, a map of the absorption density within the object can be constructed from a suitable set of projections.

beams (Fig. 1). In practice, it is the inverse Radon transform that is of particular interest:

$$f(x, y) = \int p(x \cos \phi + y \sin \phi, \phi) d\phi. \quad [2]$$

It is used to reconstruct an image from a set of projections. Note that for an object consisting of a continuous distribution of absorption intensities, the reconstruction only works if there is a large number of values of the angle  $\phi$ .

The inverse Radon transform has proved its worth in several fields—electron microscopy, geophysical exploration, and for imaging by ultrasound, X-rays and magnetic resonance, but to the best of our knowledge, it has not been applied to high-resolution NMR spectroscopy. Consider just one typical application. The computed tomography (CT) scanner irradiates the patient with parallel beams of X-rays and records a projection of the integrated absorption intensities. Then, it repeats this measurement for a series of different angles of incidence at regular intervals

around a circle. This provides enough information to permit the reconstruction of a physiological image, using the inverse Radon transform or its equivalent.

Now, imagine a different scenario. A surveyor is given the task of making a map of the distribution of trees in a small coppice. Instead of systematically logging the coordinates of each tree one-by-one, he decides to take photographs. As soon as he has set up the camera for the first shot he realizes the fundamental problem—a tree in the foreground is obscuring some more distant ones. He solves this particular local difficulty by moving the camera laterally and taking a second shot but finds that this involves some new instances of overlap. His solution is to record a complete set of photographs from different viewpoints around a circle, on the expectation that these projections will provide enough spatial information to reconstruct the desired map. The crucial point is that the object to be imaged is made up of discrete entities rather sparsely distributed, in contrast to the continuous nature of an anatomical sample examined by the CT scanner.

## RECONSTRUCTION OF MULTIDIMENSIONAL NMR SPECTRA

If we now think of a multidimensional NMR spectrum as the “object,” it has this same intrinsic property—the resonance absorptions are discrete and narrow and they are surrounded by extensive regions of space. This makes the reconstruction problem fundamentally simpler than anatomical imaging, suggesting that a rather small number of independent projections may suffice. The conventional methodology would systematically explore the time-domain data array one point at a time, equivalent to mapping frequency space one pixel at a time on a Cartesian grid. The realization that this is not the most efficient mode of data gathering has led several authors (3–18) to explore alternative methods, many of which are related in one way or another to the Radon transform.

Consider for simplicity a three-dimensional problem. The raw time-domain data are recorded at coordinates on a *polar* diagram—the essence of the Radon procedure. The corresponding *tilted* projections are derived by Fourier transformation of signals acquired while the evolution times  $t_1$  and  $t_2$  are incremented simultaneously and in a suitable ratio  $\Delta t_2 / \Delta t_1 = \tan \phi$ . The angle  $\phi$  is varied by changing this ratio. This is a consequence of a standard Fourier transform theorem (19), which states that a section through the origin of a time-domain signal  $S(t_1, t_2)$  at an angle  $\phi$  transforms as the projection of the corre-

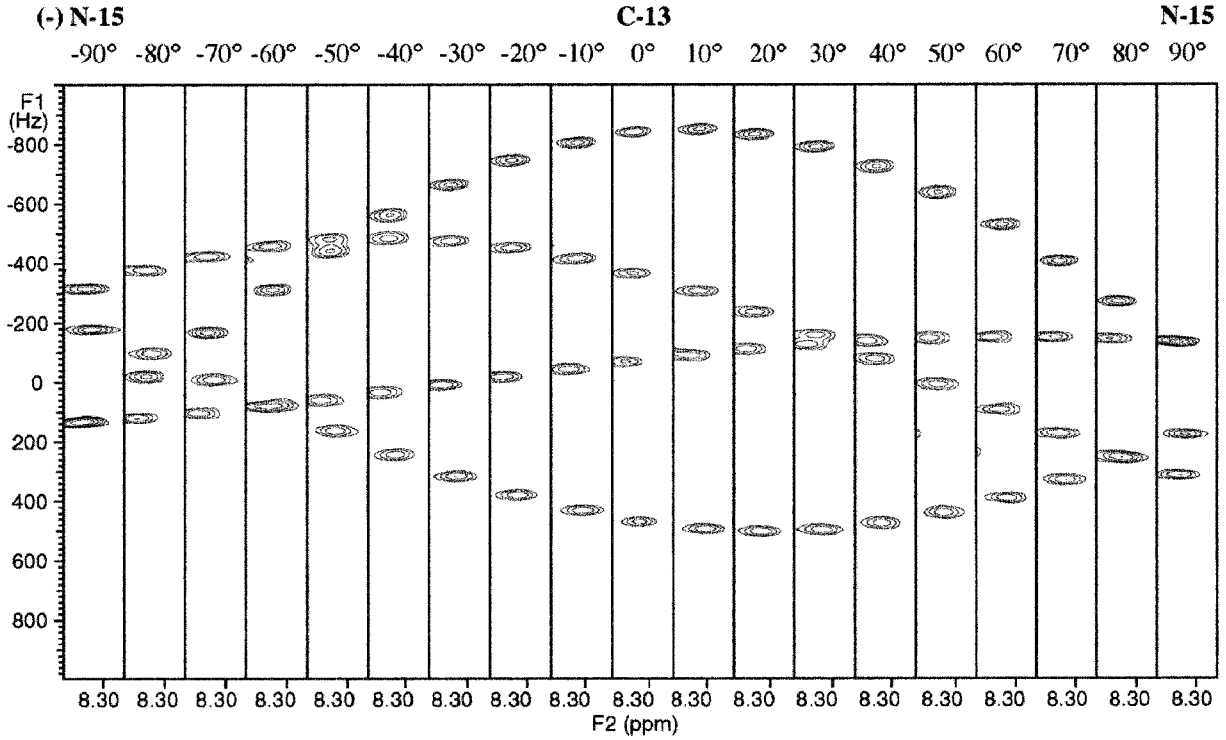


**Figure 2** Projections of selected strips from the three-dimensional NMR spectrum of isotopically enriched ubiquitin onto planes that are progressively tilted in  $10^\circ$  steps between the N-H and C-H planes. These “sinograms” would constitute the raw data for the inverse Radon transform used to reconstruct the full three-dimensional spectrum. They show how a range of different viewpoints serves to pinpoint cross-peaks even in relatively crowded spectra.

sponding frequency-domain signal  $S(F_1, F_2)$  onto an axis inclined at the same angle  $\phi$ .

In practice, the projections are obtained in pairs as a result of intermodulation of the chemical shift frequencies. Coherence that evolves in the  $t_1$  dimension ( $t_1 = t \cos \phi$ ) at a frequency  $\delta_A$  transfers a magnetization component proportional to  $\cos(2\pi\delta_A t \cos \phi)$  to the  $t_2$  dimension ( $t_2 = t \sin \phi$ ), where it then evolves at a new chemical shift frequency  $\delta_B$ . The component finally transferred to the detection stage  $t_3$  thus is modulated as

$$M_1 = \cos(2\pi\delta_A t \cos \phi) \cos(2\pi\delta_B t \sin \phi). \quad [3]$$

Complex signals are excited in both the  $t_1$  and the  $t_2$  dimensions, generating the additional sine-modulated components:

$$M_2 = \sin(2\pi\delta_A t \cos \phi) \cos(2\pi\delta_B t \sin \phi) \quad [4]$$

$$M_3 = \cos(2\pi\delta_A t \cos \phi) \sin(2\pi\delta_B t \sin \phi) \quad [5]$$

$$M_4 = \sin(2\pi\delta_A t \cos \phi) \sin(2\pi\delta_B t \sin \phi) \quad [6]$$

The usual hypercomplex Fourier transformation is derived from  $M_1 + M_4$  and  $M_2 - M_3$ :

$$\text{Re} = \cos(2\pi\delta_A \cos \phi - 2\pi\delta_B \sin \phi) \quad [7]$$

$$\text{Im} = \sin(2\pi\delta_A \cos \phi - 2\pi\delta_B \sin \phi), \quad [8]$$

which gives the difference frequency  $2\pi\delta_A \cos \phi - 2\pi\delta_B \sin \phi$ . The same data set gives the complex conjugate by negating the  $\sin \phi$  terms:

$$\text{Re} = \cos(2\pi\delta_A \cos \phi + 2\pi\delta_B \sin \phi) \quad [9]$$

$$\text{Im} = \sin(2\pi\delta_A \cos \phi + 2\pi\delta_B \sin \phi), \quad [10]$$

which gives the sum frequency  $2\pi\delta_A \cos \phi + 2\pi\delta_B \sin \phi$ . This explains why projections always occur in pairs tilted at  $\pm\phi$ . The factors  $\cos \phi$  and  $\sin \phi$  simply reflect the tilting effect.

This treatment is related to the G-matrix Fourier transform GFT-NMR method (5), but with the important generalization to all possible tilt angles, achieved by differential rates of incrementation in the

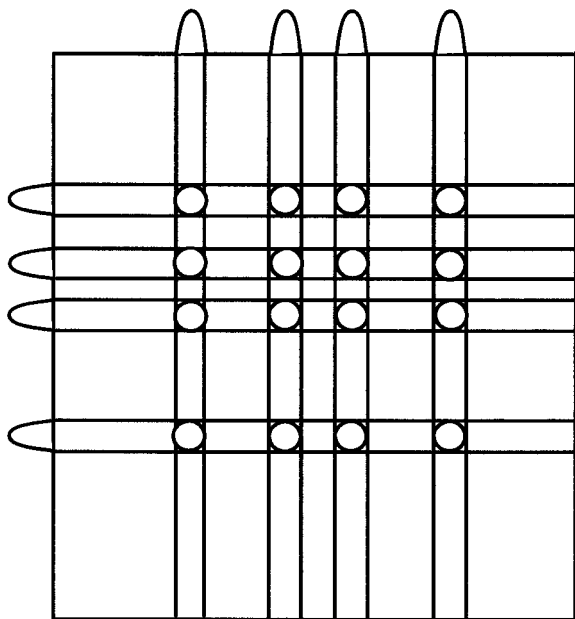


**Figure 3** When a two-dimensional NMR spectrum shows four projected peaks on each of two orthogonal axes, there are 16 *potential* cross-peak positions (circles). But because the problem is underdetermined, some of these may be false cross-peaks (zero intensity). Further information is required to solve the problem unambiguously.

various evolution dimensions. There are minor practical advantages to be gained by including projections measured at  $\phi = 0$  and  $90^\circ$ , obtained by varying only one of the evolution intervals at a time—the so-called “first planes” of the three-dimensional spectrum. Otherwise, there is no need to vary  $\phi$  in regular intervals and no particular reason to choose  $\phi = 45^\circ$ . A program can be written to predict values of  $\phi$  that minimize the incidence of overlap along the projection beams.

### Reconstruction Procedures

There are several ways to implement the inverse Radon transform. These “back-projection” techniques recreate the spectrum from so-called “sinograms”—data sampled according to the Radon scheme. Figure 2 shows sinograms obtained in a three-dimensional NMR experiment that records the correlations between carbon-13, nitrogen-15 and protons in an isotopically enriched sample of ubiquitin. As the angle  $\phi$  is varied in  $10^\circ$  steps, each individual resonance follows a unique sinusoidal trajectory, suggesting that the full spectrum is sufficiently well-defined by this limited set of observations.

We have explored a reconstruction scheme (12) based on the superposition of back-projections, pro-

cessing the multidimensional spectrum one plane at a time. In a given plane, the one-dimensional projection profile is extended at right angles, forming a set of parallel ridges. Suppose that projections have been measured on two orthogonal axes, with four absorption peaks along each axis (Fig. 3). These back-projection maps then are superimposed and compared, pixel by pixel, using an algorithm that calculates the lowest intensity at each pixel (12, 20, 21). This reduces intensities to within the baseplane noise except at the 16 intersections. These represent *potential* cross-peaks (the circles), but because the problem is underdetermined at this stage, not all of these are true cross-peaks. Now a tilted projection is measured (Fig. 4) and the lower-value algorithm is reapplied so that some of the potential cross-peaks are eliminated, leaving only five. Another projection tilted at a different angle would refine the solution further, and because of the discrete nature of the NMR resonances, the problem converges very rapidly. For a two-dimensional array, as few as three values of  $\phi$  often suffice to define all the peaks unambiguously; more values of  $\phi$  can be used for particularly crowded spectra.

A common alternative approach is to *add* the contributions from several back-projections, so that they reinforce in regions where there is strong absorption

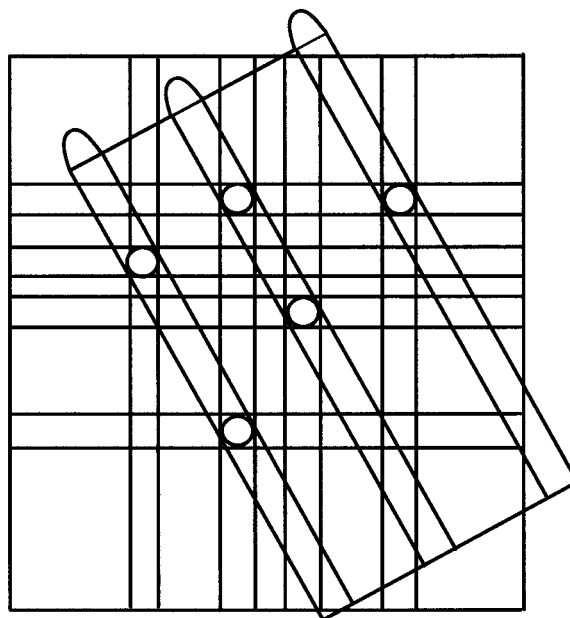
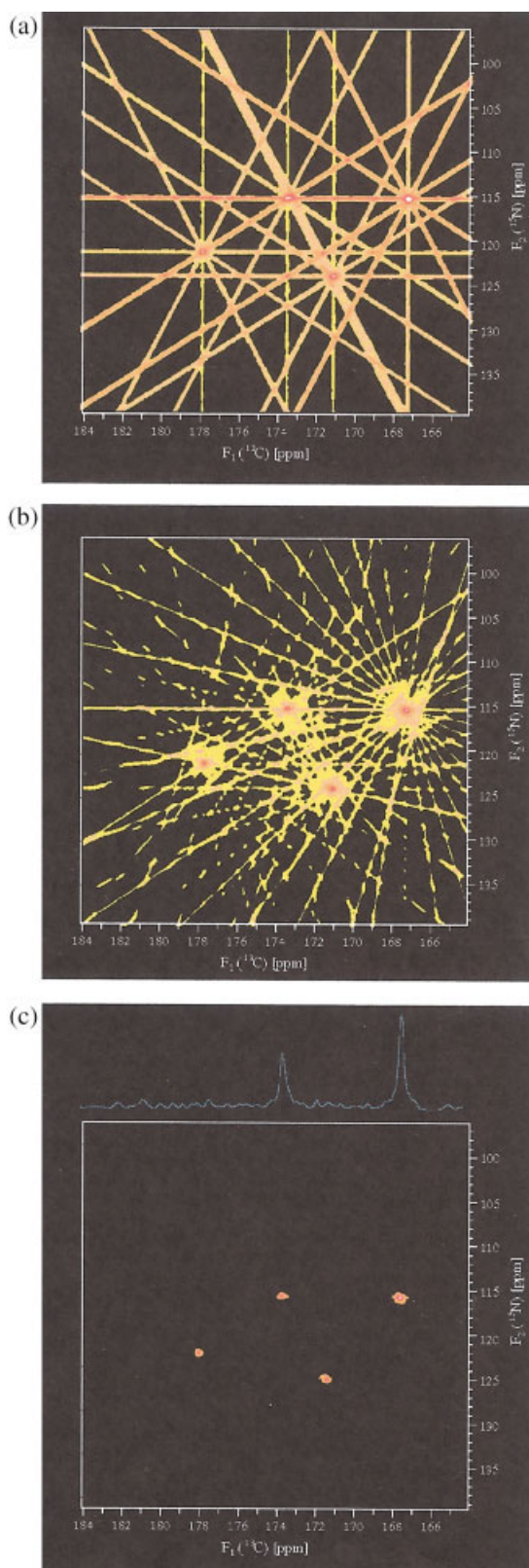


**Figure 4** A tilted projection of the spectrum shown in Fig. 3 indicates that 11 of the potential cross-peaks are false because they are not compatible with this new projection. In principle, further tilted projections might be required to confirm the validity of the remaining five peaks, but in practice the problem converges very rapidly.



in the sample. This improves the signal-to-noise ratio through the equivalent of multiscan averaging, but introduces artifacts—a set of undesirable ridges and weak “ghost” peaks where these ridges cross. The relative amplitude of these artifacts diminishes as the number of different projections is increased. This can be appreciated from Fig. 5, which compares the results of adding 6 and then 18 back-projections. In each case, the “eye of faith” would identify the genuine cross-peaks as the features with the highest intensities, but clearly 18 projections provide the more convincing picture, especially when the contours are set above the level of the artifacts. Note, however, that the speed factor favors the smallest possible number of independent projections.

Such a strict economy of data collection ensures that the full spectrum can be retrieved in a very short time. This is the major advantage over the traditional method of multidimensional NMR spectroscopy, where the spectrometer may be monopolized for days at a time by a single investigation. It is particularly important for the study of proteins, where the sample may be unstable, or where dynamic behavior is being investigated, or chemical exchange is involved. Four- and even five-dimensional NMR measurements have become popular for structural investigations, and the speed benefits derived from projection-reconstruction increase by an order of magnitude with each new frequency dimension.

Take, for example, the four-dimensional case, in which the conventional methodology systematically monitors the evolution dimensions  $t_1$ ,  $t_2$ , and  $t_3$  with  $K$ ,  $L$ , and  $M$ , increments, respectively. Although care is always taken to keep  $K$ ,  $L$ , and  $M$  as small as possible, compatible with the resolution requirements, the product  $KLM$  is unlikely to be less than about  $2^{13}$  in practice, and may need to be appreciably increased for complex spectra at high magnetic fields. In contrast, the inverse Radon transform may well permit reconstruction of the spectrum on the basis of as few as eight different projections, giving a time saving of  $2^{10}$ , that is to say, an order of magnitude for each evolution dimension. That implies a week-long exper-

**Figure 5** The inverse Radon transform. Reconstruction of the cross-peaks in a typical plane of the 600-MHz three-dimensional HNCO spectrum of ubiquitin, based on the addition of back-projections. (a) Starting with only six projections at  $0$ ,  $\pm 30$ ,  $\pm 60$ , and  $90^\circ$ , the artifactual ridges are shown clearly. (b) With 18 projections at  $0$ ,  $\pm 10$ ,  $\pm 20$ ,  $\pm 30$ ,  $\pm 40$ ,  $\pm 50$ ,  $\pm 60$ ,  $\pm 70$ ,  $\pm 80$ , and  $90^\circ$ , the ridges are less obtrusive. (c) The same spectrum as panel (b) but with contours set above the level of the artifacts. The trace indicates the signal-to-artifact ratio.

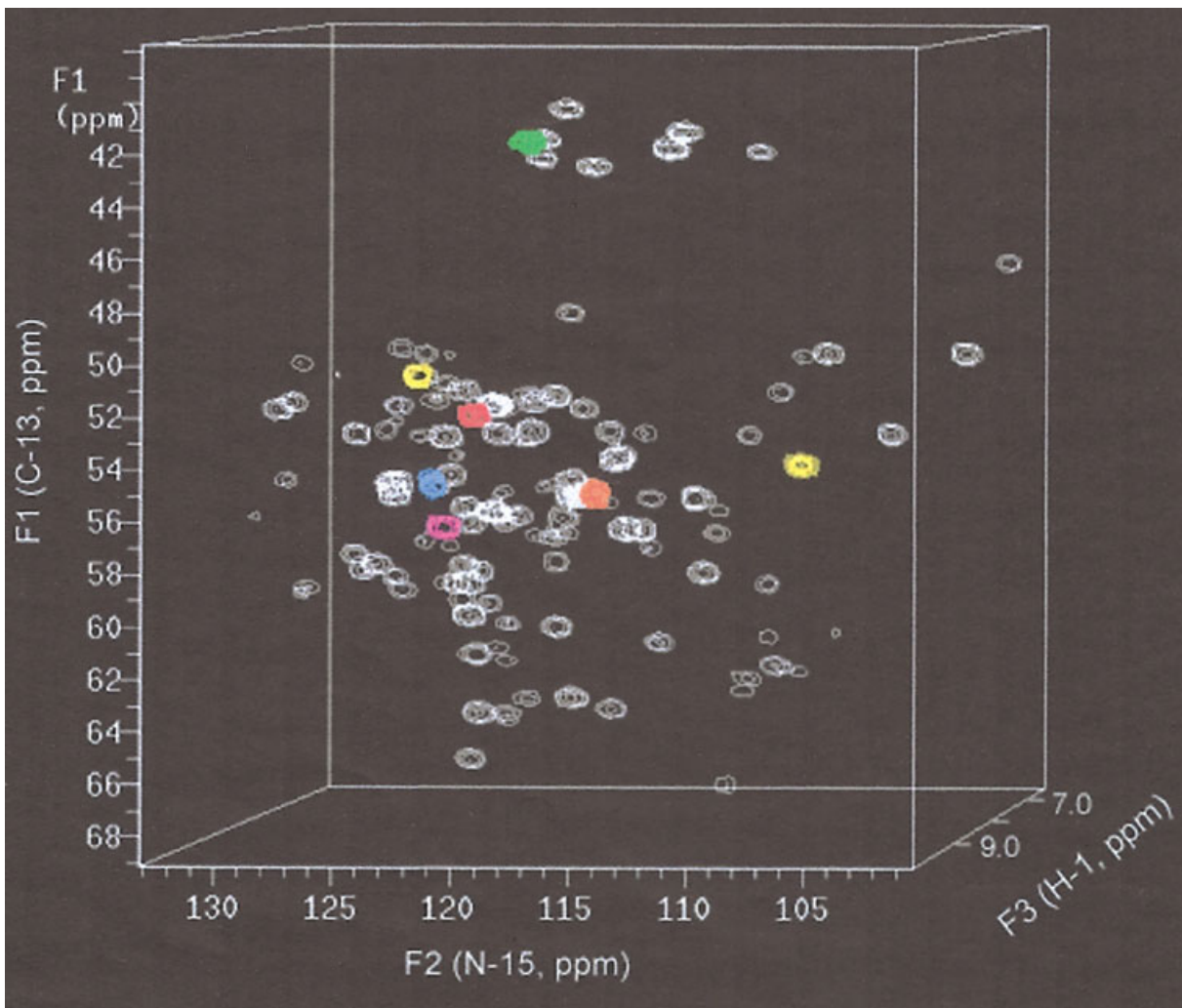


**Figure 6** A perspective representation of part of the 600-MHz three-dimensional HN(CO)CA spectrum of the isotopically-enriched 143-residue protein nuclease A inhibitor (22) showing correlations between protons, nitrogen-15, and carbon-13  $C\alpha$ -groups. Additional assignment information was obtained in the form of the carbonyl frequencies observed in the reconstructed four-dimensional HNCOCA spectrum. Seven peaks are highlighted in a plane corresponding to a proton frequency of 8.47 ppm—color-coded green for carbonyl at 178.10 ppm, magenta at 175.40 ppm, yellow at 174.45 ppm, orange at 173.04 ppm, red at 171.40 ppm, and blue at 168.27 ppm. The two peaks colored yellow have degenerate carbonyl frequencies but can be separated through their different nitrogen-15 frequencies.

iment reduced to only minutes of signal acquisition. Each further evolution dimension would require at least 16 new data acquisitions, whereas the reconstruction method only doubles the number of projections.

Projection-reconstruction NMR (“PR-NMR”) enjoys the same sensitivity per unit time as conventional methods of operation, but, as in all such measurements, the overall sensitivity falls off as the square root of the experimental duration. Fortunately, modern high-field NMR spectrometers have improved

sensitivity, particularly those equipped with a cryogenic receiver coil. Sometimes, some of the speed advantage of PR-NMR may have to be sacrificed in order to boost the sensitivity.

#### APPLICATION TO PROTEIN NMR

We illustrate the new technique by reference to part of the 600-MHz NMR spectra of a 3-mM aqueous solution (10%  $D_2O$ ) of the nuclease A inhibitor (22), a

143-residue protein. Good sensitivity is important for these experiments because multiscan averaging would reduce the speed advantage. For this reason, we used a cryogenic receiver coil cooled to 25 K to improve the signal-to-noise ratio. The three-dimensional spectrum was recorded by a standard radiofrequency pulse sequence (23) designed to correlate the chemical shifts of nitrogen-15 and carbon-13 of the  $C\alpha$ -groups with those of protons [the so-called HN(CO)CA experiment]. It used conventional methodology where both evolution dimensions  $t_1$  and  $t_2$  were sampled systematically using 64 and 32 increments, with two scans per increment, and it required 5 h and 27 min of data collection. Figure 6 displays the full three-dimensional spectrum.

This three-dimensional mode suffers from ambiguities in assignment. The accepted solution is to introduce a fourth frequency dimension where the NMR signals evolve as a function of the carbonyl frequencies, the HNCOCA experiment (24). Normally, this would place unreasonable demands on spectrometer time, but by restricting the acquisition stage to just a few projections, the PR-NMR measurements were completed in just 35 min. This was made up of 5 min each for three "orthogonal" projections obtained by varying the evolution intervals one at a time, keeping the other two at zero. It required another 20 min to record four projections tilted at  $\phi_1 = \pm 30^\circ$  in the  $F_1F_2$  plane and further tilted through  $\phi_2 = \pm 60^\circ$  out of this plane. These doubly tilted projections (17) were obtained by varying the three evolution intervals simultaneously at rates  $t_1:t_2:t_3$  in the ratios 0.433:0.250:0.866. Two scans were coadded for purposes of water suppression. It is estimated that the same spectrum recorded by the conventional method would have required roughly 4 days of data acquisition.

The three-dimensional HN(CO)CA spectrum can be rendered as a perspective display (Fig. 6). From this three-dimensional array, we selected a typical plane corresponding to a proton resonance frequency of 8.47 ppm. It comprises seven different responses representing correlations between  $C\alpha$  and nitrogen-15 sites, but at this stage, these responses can not be assigned. The solution is to exploit the associated carbonyl frequencies derived from the *four-dimensional* PR-NMR spectrum reconstructed using the equivalent of the inverse Radon transform. We chose to highlight these new assignments by color-coding the seven peaks in question on the perspective display of the three-dimensional spectrum (Fig. 6). This procedure then would be repeated for the remaining signal-bearing planes until all the peaks in the three-dimensional HN(CO)CA spectrum were properly assigned.

## CONCLUSIONS

Reconstruction of multidimensional spectra from projections involves the inverse Radon transform, a mathematical procedure not previously used in high-resolution NMR spectroscopy. Results presented here indicate that NMR information dispersed in four independent frequency dimensions can be acquired in a matter of minutes by measuring projections onto a few suitably chosen planes. This contrasts with the conventional methodology, where all three evolution dimensions must be examined independently and with fine definition—an extremely time-consuming operation. It is difficult to justify experiments that monopolize the NMR spectrometer for several days at a time. Five-dimensional experiments can be implemented by a straightforward extension of these principles, offering a time saving predicted to increase by a further order of magnitude compared with the traditional methodology. Protein studies are expected to benefit dramatically from this new approach.

## ACKNOWLEDGMENTS

The authors thank Thomas W. Kirby, Eugene F. DeRose, Geoffrey A. Mueller, Gregor Meiss, Alfred Pingoud, and Robert E. London for the sample of nuclease A inhibitor and George Gray for permission to use the Varian 600 MHz spectrometer in Palo Alto, CA.

## REFERENCES

1. Ernst RR, Anderson WA. 1966. Application of Fourier transform spectroscopy to magnetic resonance. *Rev Sci Instrum* 37:93.
2. Deans SR. 1992. *The Radon Transform and Some of Its Applications*. New York: John Wiley and Sons.
3. Ding K, Gronenborn A. 2002. Novel 2D triple-resonance NMR experiments for sequential resonance assignments of proteins. *J Magn Reson* 156: 262–268.
4. Frydman L, Scherf T, Lupulescu A. 2002. The acquisition of multidimensional NMR spectra within a single scan. *Proc Natl Acad Sci USA* 99:15859–15862.
5. Kim S, Szyperski T. 2003. GFT NMR, a new approach to rapidly obtain precise high-dimensional NMR spectral information. *J Am Chem Soc* 125:1385–1393.
6. Frydman L, Lupulescu A, Sherf T. 2003. Principles and features of single-scan two-dimensional NMR spectroscopy. *J Am Chem Soc* 125:9204–9217.
7. Chen J, De Angelis AA, Mandelshtam VA, Shaka AJ. 2003. Progress on the two-dimensional filter diagonal-

- ization method. An efficient doubling scheme for two-dimensional constant-time NMR. *J Magn Reson* 162:74–89.
8. Kupče E, Freeman R. 2003. Fast multidimensional Hadamard spectroscopy. *J Magn Reson* 163:56–63.
  9. Kupče E, Freeman R. 2003. Fast multi-dimensional NMR of proteins. *J Biomol NMR* 25:349–354.
  10. Kozminski W, Zhukov I. 2003. Multiple quadrature detection in reduced dimensionality experiments. *J Biomol NMR* 26:157–166.
  11. Freeman R, Kupče E. 2003. New methods for fast multidimensional NMR. *J Biomol NMR* 27:101–113.
  12. Kupče E, Freeman R. 2003. Reconstruction of the three-dimensional NMR spectrum of a protein from a set of plane projections. *J Biomol NMR* 27:383–387.
  13. Loening NM, Thrippleton MJ, Keeler J, Griffin RG. 2003. Single-scan longitudinal relaxation measurements in high-resolution NMR spectroscopy. *J Magn Reson* 164:321–328.
  14. Thrippleton MJ, Loening NM, Keeler J. 2003. A fast method for the measurement of diffusion coefficients: One-dimensional DOSY. *Magn Reson Chem* 41:441–447.
  15. Pelupessy P. 2003. Adiabatic single-scan two-dimensional NMR spectroscopy. *J Am Chem Soc* 125:12345–12350.
  16. Kupče E, Freeman R. 2003. Projection-reconstruction of three-dimensional NMR spectra. *J Am Chem Soc* 125:13958–13959.
  17. Kupče E, Freeman R. 2004. Fast reconstruction of four-dimensional NMR spectra from plane projections. *J Biomol NMR* 28:391–395.
  18. Lippens G, Bodart PR, Taulelle F, Amoureux, J-P. 2003. Using ANAFOR processing for a restricted least square treatment of heteronuclear spectra of biomolecules. *J Magn Reson* 161:174–182.
  19. Nagayama K, Bachmann P, Wüthrich K, Ernst RR. 1978. The use of cross-sections and of projections in two-dimensional NMR spectroscopy. *J Magn Reson* 31:133.
  20. Baumann R, Wider G, Ernst RR, Wüthrich K. 1981. Improvement of 2D NOE and 2D correlated spectra by symmetrization. *J Magn Reson* 44:402.
  21. McIntyre L, Wu X-L, Freeman R. 1990. Fine structure of cross-peaks in truncated COSY experiments. *J Magn Reson* 87:194–201.
  22. Kirby TW, DeRose EF, Mueller GA, Meiss G, Pingoud A, London RE. 2002. The nuclease A inhibitor represents a new variation of the rare PR-1 fold. *J Mol Biol* 320:771–782.
  23. Yamazaki T, Lee W, Arrowsmith CH, Muhandiram DR, Kay LE. 1994. A suite of triple resonance NMR experiments for the backbone assignment of  $^{15}\text{N}$ ,  $^{13}\text{C}$ ,  $^2\text{H}$ -labelled proteins with high sensitivity. *J Am Chem Soc* 116:11655–11666.
  24. Yang D, Kay LE. 1999. TROSY triple-resonance four-dimensional NMR spectroscopy of a 46 ns tumbling protein. *J Am Chem Soc* 121:2571–2575.

## BIOGRAPHY



**Eriks Kupče** was born in Saldus, Latvia. He received his Ph.D. (1984) and D.Sc (1989) degrees in NMR of organometallics at the Institute of Organic Synthesis in Riga. He became the youngest member of the Latvian Academy of Sciences in 1990. In the same year, he surfed the first wave of Soviet post-docs going west, won the Humboldt Fellowship, and worked with Prof. B. Wrackmeyer in Bayreuth, Germany. From 1991 to 1992 he received training in spin-gymnastics at Cambridge University from Prof. Ray Freeman. In 1993 he moved to Oxford University, reversing the “forbidden transition” of his supervisor and joined the laboratory of Iain Campbell. Currently, he is the Principal Scientist at Varian, Inc., in Oxford, U.K. His most recent research involves the design and

applications of selective pulses; adiabatic decoupling and mixing; signal processing; fast NMR techniques, particularly Hadamard spectroscopy; and the projection-reconstruction method.



**Ray Freeman** is a graduate of Oxford University, where he studied for his doctorate under Rex Richards. After his postdoctoral research with Anatole Abragam and Robert Pound in Paris, he joined the National Physical Laboratory in Teddington, U.K., before moving to Varian Associates in Palo Alto, CA. He returned to Oxford University in 1973 to build a research group working on high-resolution NMR methodology, particularly two-dimensional spectroscopy. In 1987, he made the forbidden transition to Cambridge University. Dr. Freeman formally retired in 1999.